

Accessible and informative sectioned images and surface models of the maxillofacial area for orthognathic surgery

B.C. Kim^{1, 2}, M.S. Chung², H.S. Park³, D.S. Shin⁴, J.S. Park³

¹Department of Oral and Maxillofacial Surgery, Daejeon Dental Hospital, Wonkwang University College of Dentistry, Daejeon, Korea

²Department of Anatomy, Ajou University School of Medicine, Suwon, Korea

³Department of Anatomy, Dongguk University School of Medicine, Gyeongju, Korea

⁴Department of Orthopaedic Biomaterial Science, Osaka University Graduate School of Medicine, Osaka, Japan

[Received 11 November 2014; Accepted 12 December 2014]

Background: The aim of this study was to describe sectioned images and stereoscopic anatomic models of the maxillofacial area by using Visible Korean which are beneficial for medical education and clinical training in the field of orthognathic surgery.

Materials and methods: Serially sectioned images of the maxillofacial area of a cadaver were created. Significant structures in the sectioned images were outlined and stacked to build surface models.

Results: Browsing software (95.1 MB) and portable document format (PDF) file (142 MB) that were constructed are freely downloadable from our website (<http://anatomy.co.kr>). In the browsing software, the names of structures associated with malocclusion and orthognathic surgery could be viewed on the sectioned images. In the PDF file, surface models and stereoscopic maxillofacial structures were displayed in real-time.

Conclusions: The state-of-the-art sectioned images, outlined images, and surface models that were arranged and systematised in this study, may help students and trainees investigate the anatomy of the maxillofacial area for orthognathic surgery. (Folia Morphol 2015; 74, 3: 346–351)

Key words: orthognathic surgery, three-dimensional, visible human projects

INTRODUCTION

Craniofacial dysmorphism is characterised by functional and structural imbalances of the face [6, 7]. This dysmorphism has diverse aspects such as malocclusion, asymmetry, apertognathia, retrognathism, or prognathism. Therefore, patients with these developmental deformities often need operative intervention such as orthognathic surgery. Unfortunately, a potential risk of damage to vital structures such as nerve injury or vessel perforation during these procedures can occur

to a surgeon involved in the treatment of a patient with craniofacial dysmorphism [8, 9, 17]. How to avoid and manage these complications provides practitioners with successful results. To become a skilful surgeon for this orthognathic surgery, anatomical knowledge of the maxillofacial area is profitable and it is surely necessary to experience many cases of operation. However, it is not easy to understand the stereoscopic shape of the anatomic structures and accumulate knowhow of surgery thoroughly in a short period.

Address for correspondence: J.S. Park, PhD, Department of Anatomy, Dongguk University School of Medicine, 87 Dongdae-ro, Gyeongju, 780-350, Republic of Korea, e-mail: park93@dongguk.ac.kr

Table 1. 113 outlined structures and surface models of maxillofacial area

Systems (no. of structures)	Structures
Skeletal (29)	Cranium without mandible*†, Pterygoid fissure*, Pterygoid plate*, Nasal bone†, Vomer†, Maxilla†, Maxillary sinus*, Zygomatic bone*†, Mandible†, Mental foramen*, Lingula*, Antilingula eminence*, Mandibular notch*, Antegonial notch*, External oblique ridge*, Hyoid bone†, Inferior nasal concha*†
Digestive (33)	Buccal fat pad*, Maxillary central incisor*, Maxillary lateral incisor*, Maxillary canine*, Maxillary first premolar*, Maxillary second premolar*, Maxillary first molar*, Maxillary second molar*, Mandibular central incisor*, Mandibular lateral incisor*, Mandibular canine*, Mandibular first premolar*, Mandibular second premolar*, Mandibular first molar*, Mandibular second molar*, Mandibular third molar*, Tongue†
Muscular (16)	Nasalis musclet, Orbicularis oris musclet, Masseter muscle*†, Temporal muscle*†, Lateral pterygoid muscle*†, Medial pterygoid muscle*†, Digastric muscle*†, Stylohyoid muscle*†, Mylohyoid muscle*†
Cardiovascular (27)	Common carotid artery*†, External carotid artery*†, Facial artery*, Maxillary artery*, Inferior alveolar artery*, Descending palatine artery*, Greater palatine artery*, Nasopalatine artery, Internal carotid artery*†, Internal jugular vein*†, Facial vein*, Retromandibular vein*†, External jugular vein*†, Pterygoid plexus*
Nervous (6)	Lingual nerve*, Inferior alveolar nerve*, Mental nerve*
Integumentary (2)	Skin*†

*Bilateral structures were surface reconstructed; †Structures outlined in our previous studies [21]

Recent advances in computer graphic technology has resulted in the development of virtual three-dimensional (3D) dissection software that is primarily based on computed tomography (CT), magnetic resonance image (MRI), and sectioned images [1, 3, 10, 11]. This 3D software is of helpful to a student or a common user. However, it is not applicable to the operative patterns of surgical approaches, because it focuses on teaching anatomy. Furthermore, it is difficult for CT or MRI to describe it in detail because the anatomy of the maxillofacial area is complicated and is more complex by small size of the adjacent structures [10]. Therefore cross sectional images of the colour version, the resolution of which was higher than CT or MRI, were needed to create stereoscopic images that are helpful in surgery.

The purpose of this study was to represent state-of-art sectioned images and surface models of the maxillofacial area which were beneficial for medical education and clinical training in the field of orthognathic surgery. Another aim was to describe the browsing software and portable document format (PDF) file which enabled a user to access sectioned images easily and to access surface models of our datasets, respectively. Maxillofacial surgeons may be able to assess the complete data, with the aim of understanding the anatomy of the maxillofacial area and improving the surgical outcome. In addition,

a comprehensive knowledge of maxillofacial anatomy may maximise the surgical predictability and avoid unfavourable complications. Moreover, virtual orthognathic surgery could be achieved by using the PDF file of this study.

MATERIALS AND METHODS

Outlining of the sectioned images

We had already created the sectioned images (intervals, 0.1 mm; pixel size, 0.1 mm; colour depth, 48 bit colour; file format, tagged image file format [TIFF]) and colour-filled images (intervals, 1.0 mm; pixel size, 0.1 mm; colour depth, 8 bit colour; file format, TIFF) of a cadaver head [14, 21]. Partial structures of the maxillofacial area were previously outlined and we selectively include them to meet the interest of orthognathic surgery (Table 1).

We additionally made colour images of maxillofacial structures associated with malocclusion and orthognathic surgery (i.e., inferior alveolar nerve) manually on Photoshop CS5 (Adobe Systems, Inc., San Jose, CA, USA) with a lasso tool at 1.0 mm or 0.5 mm intervals (Table 1). If adjacent up-and-down outlines of a structure did not overlap, the continuity of the outline was broken in the reconstructed surface models. Therefore, we duplicated the outline of the adjacent previous layer, and then pasted it on the

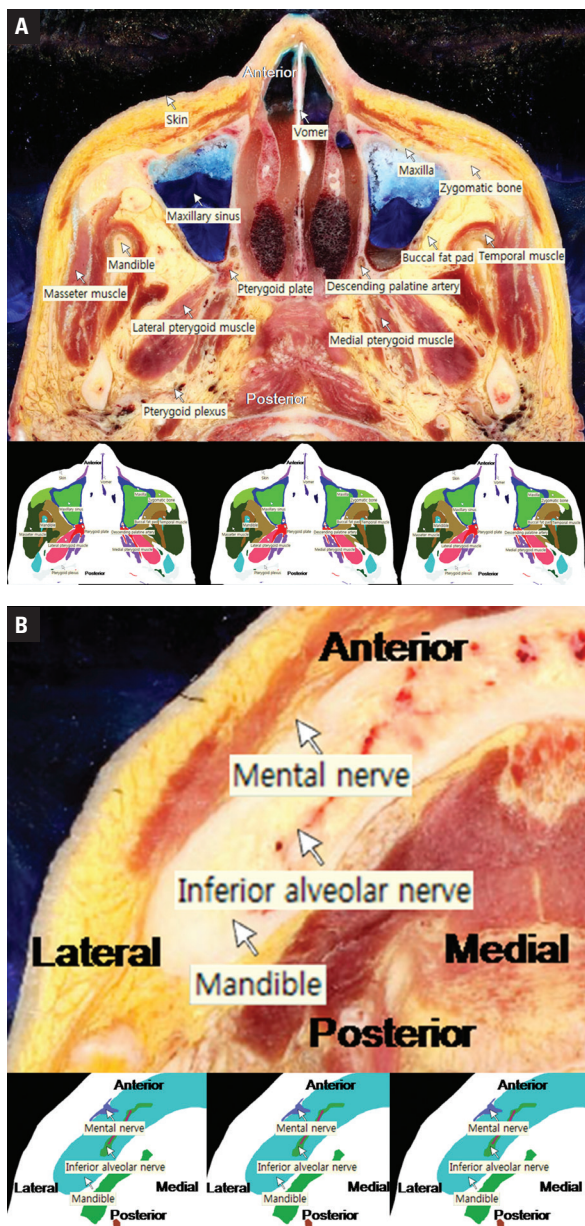


Figure 1. Browsing software of maxillofacial area. The name of each structure is displayed when the mouse pointer indicates a specific structure; **A.** Sectional and colour-filled images of maxilla; **B.** Sectional and colour-filled images of mandible.

layer in progress. We also compared the structures of the ongoing layer with the previous layer. In this way, we outlined the sectioned images one by one. All outlines of each structure were then filled with a specific colour semi-automatically to make colour-filled images (pixel size, 0.1 mm; colour depth, 8-bit colour; file format, bitmap [BMP]) [4, 13, 14].

In our previous studies [5, 19, 21], browsing software was made of the sectioned and colour-filled images

using C# language of Microsoft Visual Studio, NET 2003 (Microsoft Corporation, Redmond, WA). The images of this study were put into each folder of the browsing software. And with package software, Nullsoft Scriptable Install System of NSIS Media, operating files and image folders were transformed into one installation file (file name, Orthognathic_surgery.exe) (Fig. 1) [12].

Reconstructed surface models

We constructed surface models of colour-filled images associated with orthognathic surgery for this study. As a result, a total of 113 outlined structures have been surface reconstructed (Table 1). To create surface models, Mimics version 17.0 (Materialise, Leuven, Belgium) were used. In Mimics, colour-filled images in the BMP format were opened. We regulated their thresholds. They were then stacked continuously. The surface models were painted individually or by systems to differentiate the combined structures (Table 1). The colour of skin, muscle, bone and teeth was constituted semi-transparent to display inside (Fig. 2). Improper surface models that resulted from inadequate outlining were adjusted by the maxillofacial surgeon and anatomist [4, 15, 16]. In this way, surface models were established. The formed surface models were saved as stereolithography (STL) files to be accessible on the Maya version 2012 (Autodesk, Inc., San Rafael, CA) (Fig. 2) [20, 21]. Using Maya, we performed virtual orthognathic surgery (Fig. 2).

PDF file of surface models

Using deep exploration standard (Right Hemisphere, San Ramon, CA, USA), STL files were classified into several structures and the surface models were organised in official anatomical names [2]. After the arrangement, all models in the STL files were assembled and saved as Orthognathic_surgery.pdf using the 3D Reviewer, accompanying software of Acrobat 9.0 Pro Extended (Adobe Systems, Inc., San Jose, CA, USA) [18, 20]. Because the PDF file was accessed in Adobe Reader, the anatomical names of the parts were presented in the model tree window.

In Acrobat, we assembled bookmarks of the PDF file. The bookmarks were as follows: All structures (oblique view), skin removed, muscles removed, bones removed, blood vessels removed, LeFort I osteotomy, sagittal split ramus osteotomy, intraoral vertical ramus osteotomy, genioplasty, angle reduction, anterior segmental osteotomy, and anterior subapical osteotomy (Fig. 2).

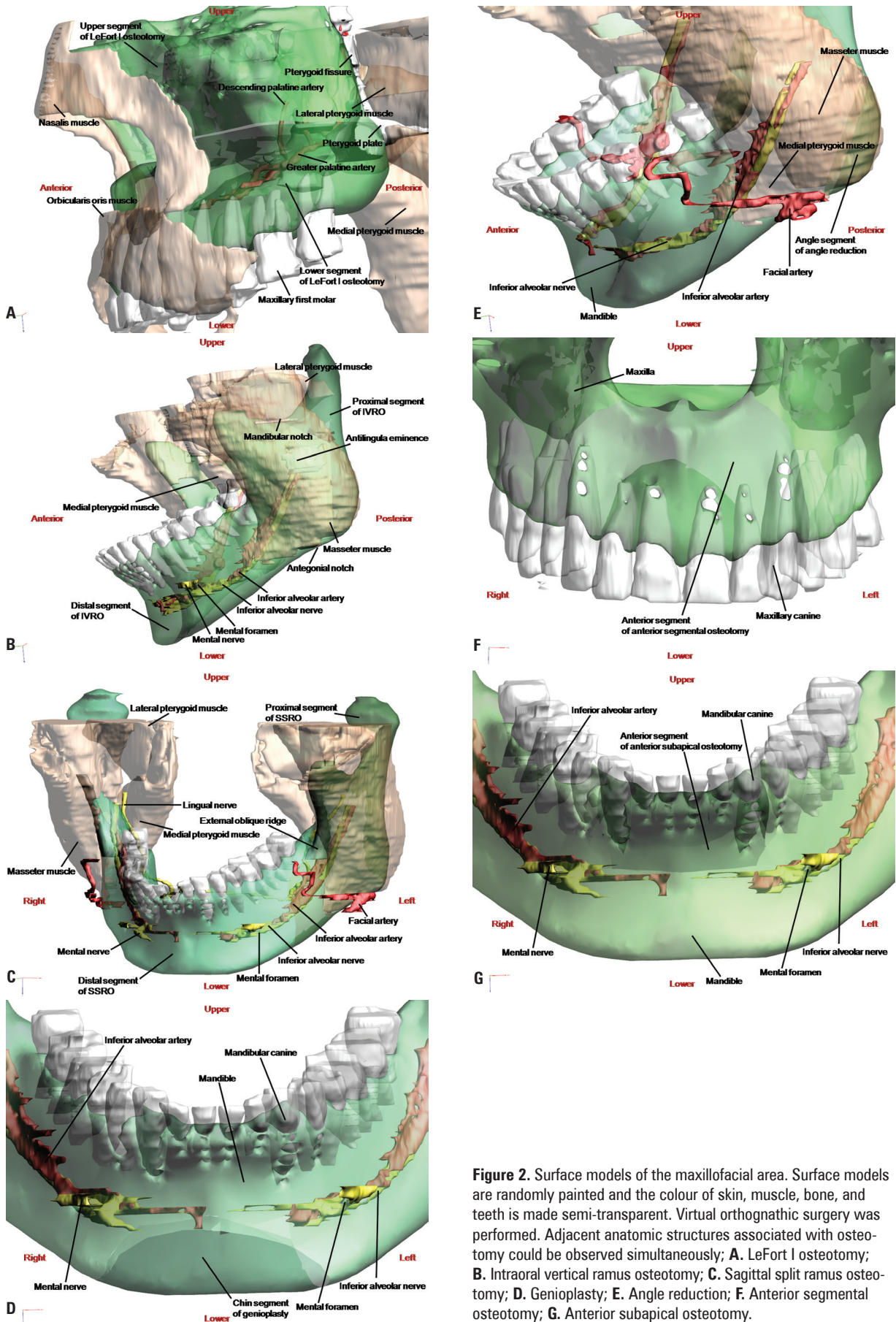


Figure 2. Surface models of the maxillofacial area. Surface models are randomly painted and the colour of skin, muscle, bone, and teeth is made semi-transparent. Virtual orthognathic surgery was performed. Adjacent anatomic structures associated with osteotomy could be observed simultaneously; **A.** LeFort I osteotomy; **B.** Intraoral vertical ramus osteotomy; **C.** Sagittal split ramus osteotomy; **D.** Genioplasty; **E.** Angle reduction; **F.** Anterior segmental osteotomy; **G.** Anterior subapical osteotomy.

RESULTS

The browsing software (file name, Orthognathic_surgery.zip; file size, 95.1 MB) and PDF file (file name, Orthognathic_surgery.pdf; file size, 142 MB) that were constructed are freely downloadable from our website (<http://anatomy.co.kr>). The files can be accessed free of charge. In the browsing software, the names of the structures associated with malocclusion and orthognathic surgery were displayed on the sectioned images. In the PDF file, the surface models, and stereoscopic maxillofacial structures were displayed in real-time. The maxillofacial anatomy could be easily perceived by investigating the sectional images of the browsing software and the surface models of the PDF file as follows.

In the browsing software, the lateral pterygoid muscle and the superficial head of the medial pterygoid muscle were attached to the maxillary posterior area (Fig. 1A). The descending palatine artery descended through the greater palatine canal and emerged from the greater palatine foramen (Fig. 1A). By considering this, a user can comprehend a damage to the medial and lateral pterygoid muscle during LeFort I osteotomy may cause intraoperative haemorrhage and maintaining the integrity of the descending palatine artery is necessary to avoid excessive bleeding. Meanwhile, the user could observe the run of the branches of mandibular nerve (Fig. 1B). Therefore, the user can understand that an inaccurate mandibular osteotomy may cause nerve damage.

In the PDF file, the sigmoid notch was displayed as a concavity on the superior surface of the mandibular ramus between the coronoid and condyloid processes and the antegonial notch was displayed as a depression on the lower edge of the mandible, near the margin of the masseter muscle attachment (Fig. 2B). The antilingula eminence could be detected on the lateral surface of the ramus (Fig. 2B). As a result, a user can understand that two Bauer retractors should be simultaneously inserted into the antegonial notch and sigmoid notch and that cutting the ramus should be performed behind the antilingula eminence in the intraoral vertical ramus osteotomy (IVRO) (Fig. 2B). In addition, the user could observe the 3D structure of the inferior alveolar nerve, mental nerve, and facial artery in the PDF file (Fig. 2C). The mandible and the adjacent muscles can be designated in a semi-transparent colour. Therefore the user might keep in mind where the osteotomy lines should be located in the sagittal split ramus

osteotomy (SSRO), angle reduction, or genioplasty (Fig. 2C–E). Meanwhile, osteotomy lines should be positioned on the interdental area to avoid damage of dental roots in anterior segmental osteotomy or anterior subapical osteotomy (Fig. 2F, G).

Based on this knowledge, virtual orthognathic surgery could be performed in the PDF file (Fig. 2). LeFort I osteotomy was performed in the maxilla. We could find the location of the buccal fat pad, pterygoid maxillary fissure, and descending palatine artery, etc. (Fig. 2A). IVRO and genioplasty were performed in the mandible (Fig. 2B, D). Adjacent structures such as the inferior alveolar nerve, mental nerve, and facial artery could be observed.

DISCUSSION

We have reported surface models of a cadaver head in a previous study [21], and they were helpful to understand the anatomical structures on the maxillofacial area. However, it did not represent vital structures of maxilla and mandible (i.e., inferior alveolar nerve). Therefore, in this study, we added a series of structures of maxillofacial area (Table 1) and described a virtual operative procedure associated with orthognathic surgery (Fig. 2) to get a better surgical outcome and reduce complications.

As to LeFort I osteotomy of the maxilla, our sectional images revealed the thinness of the maxilla and the location of the buttress (Fig. 1). Therefore, a user could recognise that strong manipulation was not required in sawing and where the osteotomes were positioned. And colour-filled images showed the medial/lateral pterygoid muscles and the pterygoid plexus (Fig. 1). A user could perceive that intraoperative bleeding of the maxilla was primarily associated with tearing of the medial/lateral pterygoid muscles, but not the pterygoid plexus [8]. Therefore almost minor haemorrhage can be managed by compression or by application of topical haemostatic agents. Our PDF file described the buccal fat pad, pterygoid plate, and descending palatine artery (Fig. 2). The buccal fat pad is posterior of the maxillary first molar and incision should be performed anterior to it to avoid the herniation of it. Meanwhile the descending palatine artery is closely located with pterygoid plate and the user keep in mind the manipulation of pterygoid plate could induce transection of descending palatine artery. In this case, vessel ligation of the source of bleeding is an appropriate approach.

In the mandibular osteotomy such as IVRO, SSRO, genioplasty, and angle reduction, sectional images

revealed the location of mandibular or mental foramen (Fig. 1). Inferior alveolar nerve enters the mandible via mandibular foramen and exits via mental foramen. Thus the user proves that osteotomy line should be located over the mandibular foramen or under the mental foramen to avoid nerve damage. And the PDF file displayed stereoscopic skeletal structures such as the lingula, antilingula eminence, mandibular notch, antegonial notch, and external oblique ridge (Fig. 2). These are indicators for an osteotomy (lingula, antilingula eminence, and external oblique ridge) or for retraction (mandibular notch and antegonial notch). Therefore a user can understand the manipulation of the saw, osteotome or retractor. The PDF file also presents the stereoscopic location of the facial artery (Fig. 2). A user can understand that care should be taken in the mandibular inferior border osteotomy of SSRO or angle reduction to prevent intraoperative bleeding.

About the segmental osteotomy such as maxillary anterior segmental or mandibular anterior subapical osteotomy, the PDF file described stereoscopic shape and position of dental roots (Fig. 2). Therefore, a user can know where the osteotomy lines should be located to inhibit the injury to the dental roots.

CONCLUSIONS

In this study, we targeted a thorough understanding of stereoscopic anatomical structure in the maxillofacial area. We hope this study contribute to better surgical outcomes for orthognathic surgery. Especially students, trainees of maxillofacial surgery may grasp the principle of orthognathic surgery.

ACKNOWLEDGEMENTS

This work (NRF-2012R1A2A2A01012808) was supported by Mid-career Researcher Program through NRF grant funded by the MEST.

REFERENCES

1. <http://www.visiblebody.com/index.html>.
2. FIPAT (2011) Terminologia Anatomica: International Anatomical Terminology. Thieme.
3. <http://www.zygotebody.com>.
4. Jang HG, Chung MS, Shin DS, Park SK, Cheon KS, Park HS, Park JS (2011) Segmentation and surface reconstruction of the detailed ear structures, identified in sectioned images. *Anat Rec (Hoboken)*, 294: 559–564.
5. Kim BC, Chung MS, Kim HJ, Park JS, Shin DS (2014) Sectioned images and surface models of a cadaver for understanding the deep circumflex iliac artery flap. *J Craniofac Surg*, 25: 626–629.
6. Kim BC, Lee CE, Park W, Kang SH, Zhengguo P, Yi CK, Lee SH (2010) Integration accuracy of digital dental models and 3-dimensional computerized tomography images by sequential point- and surface-based markerless registration. *Oral Surg Oral Med Oral Pathol Oral Radiol Endod*, 110: 370–378.
7. Kim BC, Lee CE, Park W, Kim MK, Zhengguo P, Yu HS, Yi CK, Lee SH (2011) Clinical experiences of digital model surgery and the rapid-prototyped wafer for maxillary orthognathic surgery. *Oral Surg Oral Med Oral Pathol Oral Radiol Endod*, 111: 278–285.e271.
8. Kramer FJ, Baethge C, Swennen G, Teltzrow T, Schulze A, Berten J, Brachvogel P (2004) Intra- and perioperative complications of the LeFort I osteotomy: a prospective evaluation of 1000 patients. *J Craniofac Surg*, 15: 971–977; discussion 978–979.
9. Lanigan DT, Hey J, West RA (1991) Hemorrhage following mandibular osteotomies: a report of 21 cases. *J Oral Maxillofac Surg*, 49: 713–724.
10. Liu K, Fang B, Wu Y, Li Y, Jin J, Tan L, Zhang S (2013) Anatomical education and surgical simulation based on the Chinese Visible Human: a three-dimensional virtual model of the larynx region. *Anat Sci Int*, 88: 254–258.
11. Marchetti C, Bianchi A, Muijldermans L, Di Martino M, Lancellotti L, Sarti A (2011) Validation of new soft tissue software in orthognathic surgery planning. *Int J Oral Maxillofac Surg*, 40: 26–32.
12. Park HS, Chung MS, Shin DS, Jung YW, Park JS (2013) Accessible and informative sectioned images, color-coded images, and surface models of the ear. *Anat Rec (Hoboken)*, 296: 1180–1186.
13. Park JS, Chung MS, Chi JG, Park HS, Shin DS (2010) Segmentation of cerebral gyri in the sectioned images by referring to volume model. *J Korean Med Sci*, 25: 1710–1715.
14. Park JS, Chung MS, Park HS, Shin DS, Har DH, Cho ZH, Kim YB, Han JY, Chi JG (2010) A proposal of new reference system for the standard axial, sagittal, coronal planes of brain based on the serially-sectioned images. *J Korean Med Sci*, 25: 135–141.
15. Park JS, Jung YW, Lee JW, Shin DS, Chung MS, Riemer M, Handels H (2008) Generating useful images for medical applications from the Visible Korean Human. *Comput Methods Programs Biomed*, 92: 257–266.
16. Park JS, Shin DS, Chung MS, Hwang SB, Chung J (2007) Technique of semiautomatic surface reconstruction of the visible Korean human data using commercial software. *Clin Anat*, 20: 871–879.
17. Phillips C, Essick G, Blakey G, 3rd, Tucker M (2007) Relationship between patients' perceptions of postsurgical sequelae and altered sensations after bilateral sagittal split osteotomy. *J Oral Maxillofac Surg*, 65: 597–607.
18. Puchwein P, Schildhauer TA, Schoffmann S, Heidari N, Windisch G, Pichler W (2012) Three-dimensional morphometry of the proximal ulna: a comparison to currently used anatomically preshaped ulna plates. *J Shoulder Elbow Surg*, 21: 1018–1023.
19. Shin DS, Chung MS, Park HS, Park JS, Hwang SB (2011) Browsing software of the Visible Korean data used for teaching sectional anatomy. *Anat Sci Educ*, 4: 327–332.
20. Shin DS, Chung MS, Park JS (2012) Systematized methods of surface reconstruction from the serial sectioned images of a cadaver head. *J Craniofac Surg*, 23: 190–194.
21. Shin DS, Jang HG, Park JS, Park HS, Lee S, Chung MS (2012) Accessible and informative sectioned images and surface models of a cadaver head. *J Craniofac Surg*, 23: 1176–1180.